# Finite-Difference Time-Domain Calculation of the Spontaneous Emission Coupling Factor in Optical Microcavities

Jelena Vučković, *Student Member, IEEE,* Oskar Painter, *Student Member, IEEE,* Yong Xu, Amnon Yariv, *Life Fellow, IEEE,* and Axel Scherer

***Abstract*— We present a general method for the $\beta$ factor calculation in optical microcavities. The analysis is based on the classical model for atomic transitions in a semiconductor active medium. The finite-difference time-domain method is used to evolve the electromagnetic fields of the system and calculate the total radiated energy, as well as the energy radiated into the mode of interest. We analyze the microdisk laser and compare our result with the previous theoretical and experimental analyses. We also calculate the $\beta$ factor of the microcavity based on a two-dimensional (2-D) photonic crystal in an optically thin dielectric slab. From the $\beta$ calculations, we are able to estimate the coupling to radiation modes in both the microdisk and the 2-D photonic crystal cavity, thereby showing the effectiveness of the photonic crystal in suppressing in-plane radiation modes.**

***Index Terms*—$\beta$ factor, finite-difference time-domain methods, microcavity, microdisk, photonic crystals, spontaneous emission.**

## I. Introduction

The spontaneous emission coupling factor ($\beta$ factor) of a given mode is defined as the ratio of the spontaneous emission rate into that mode and the spontaneous emission rate into all modes [1]. There are many analyses (both classical and quantum mechanical) of this parameter in the literature, but they consider only simple laser geometries and often use many approximations. These include the spontaneous emission factor of the injection laser [2], the vertical-cavity surface-emitting laser (VCSEL) of square cross section [3], [4], the microdisk [5], and the ring laser [6].

Over the past few years, much scientific attention has been focused on the use of photonic crystals [7]–[9] for building optical microcavities [10]–[12] for spontaneous emission control [13] and thresholdless lasing [1], [14]. However, due to the complex geometry of the proposed microcavities, it was not possible to perform a detailed analysis of the $\beta$ factor. Our goal is to define a method for the calculation of this important parameter which is flexible enough to incorporate highly complex geometries, including those of photonic crystals.

In Section II, we describe a method for calculating the spontaneous emission factor using the finite-difference time-domain (FDTD) method [15], [16]. In Sections III and IV, we present our results for the $\beta$ factor of the microdisk laser and of the optical microcavity incorporating a two-dimensional photonic bandgap structure (2-D PBG).

Manuscript received January 14, 1999; revised April 30, 1999. This work was supported by the National Science Foundation under Contract ECS-9632937 and by DARPA under Contract N00014-96-1-1295.

The authors are with the Electrical Engineering and Applied Physics Departments, California Institute of Technology, Pasadena, CA 91125 USA.

Publisher Item Identifier S 0018-9197(99)05960-6.

## II. Description of the Proposed Method

Our starting point is the classical model for the $\beta$ factor calculation [2]–[4]. Atomic transitions are modeled as classical oscillating electric dipoles with resonant frequencies equal to the atomic transition frequency $\omega_p$. Different dephasing mechanisms are taken into account through the dipole lifetime $\tau_d$, which corresponds to homogeneous broadening of the spontaneous emission spectrum [17].

### A. No Dipole Sources

Consider first the electromagnetic field of the system when dipoles are not present. We solve the problem in a large box, which we call the computational domain and denote $V_{CD}$. Appropriate boundary conditions, which depend on the physical situation of interest, have to be applied to the surface enclosing $V_{CD}$. We neglect the absorption losses (i.e., we assume that the conductivity of a medium is equal to zero). At any point inside the box, the set of Maxwell's curl equations has to be satisfied:

$$\vec{\nabla} \times \vec{H} = \epsilon(\vec{r})\,\frac{\partial \vec{E}}{\partial t} \tag{1}$$

$$\vec{\nabla} \times \vec{E} = -\mu_0 \frac{\partial \vec{H}}{\partial t}. \tag{2}$$

Let $\{\vec{E}_m(\vec{r})\}$ be the complete set of transverse orthonormal modes of the lossless cavity [18]–[20]. The orthonormality condition (with a position-dependent dielectric constant $\epsilon(\vec{r})$) is defined as [19]

$$\iiint_{V_{CD}} \epsilon(\vec{r})\vec{E}_m(\vec{r}) \cdot \vec{E}_n^*(\vec{r})\, d^3\vec{r} = \delta_{mn} \tag{3}$$

where $\delta_{mn}$ is the Kronecker's delta. The transversality condition is given by [19]

$$\vec{\nabla} \cdot (\epsilon(\vec{r})\vec{E}_m(\vec{r})) = 0. \tag{4}$$

Each of these modes satisfies the following wave equation:

$$\vec{\nabla} \times [\vec{\nabla} \times \vec{E}_m(\vec{r})] = \mu_0 \epsilon(\vec{r})\omega_m^2 \vec{E}_m(\vec{r}) \tag{5}$$

where $\omega_m$ is the frequency of a mode. In the mode expansion method, we express the total electric field of the cavity using the modes from the set $\{\vec{E}_m(\vec{r})\}$ [18], [19]

$$\vec{E}(\vec{r},t)=\sum_m \vec{E}_m(\vec{r})f_m(t)=\sum_m \vec{\eta}_m(\vec{r},t). \tag{6}$$

Each term $\vec{\eta}_m(\vec{r},t)$ in the previous expansion satisfies the following wave equation:

$$\vec{\nabla}\times\vec{\nabla}\times\vec{\eta}_m=-2\kappa_m\mu_0\epsilon(\vec{r})\,\frac{\partial\vec{\eta}_m}{\partial t}-\mu_0\epsilon(\vec{r})\,\frac{\partial^2\vec{\eta}_m}{\partial t^2} \tag{7}$$

where $\kappa_m$ is the field decay rate for the $m$th mode, which accounts for the radiation outside the box. For some optical mode described by frequency $\omega_m$ and the quality factor [21] $Q_m$, the field decay rate is given by

$$\kappa_m=\frac{\omega_m}{2Q_m}. \tag{8}$$

From (3), (5), and (7), it follows that

$$\ddot{f}_m(t)+2\kappa_m\dot{f}_m(t)+\omega_m^2 f_m(t)=0 \tag{9}$$

with the solution:

$$f_m(t)=F_m e^{i\omega_m' t}e^{-(\omega_m t/2Q_m)} \tag{10}$$

where $\omega_m'=\omega_m(1-(1/4Q_m^2))^{1/2}$. For the cavity modes of interest, $Q_m$ is large enough so that we can assume $\omega_m'\approxeq\omega_m$.

We can discretize space and time in (1) and (2) and use the FDTD method to calculate the electromagnetic field of the system. We apply Mur's absorbing boundary condition [22] to the boundaries of the computational domain which allows the radiation to escape outside, without reflecting back into $V_{CD}$.

The first step in our calculation involves isolating the mode of interest in the optical cavity. Starting with an initial field distribution $\vec{E}(\vec{r},t=0)$ and $\vec{H}(\vec{r},t=0)$, we use the FDTD analysis to time evolve the electric and magnetic field in $V_{CD}$. During the time evolution, we store the field at a point of low symmetry in the microcavity. After applying a fast Fourier transform (FFT) to the resulting time series, we observe the resonant peaks in the spectrum corresponding to the modes of the structure. Then we filter the electromagnetic field for the mode of interest [what we term as the fundamental mode, whose electric field is denoted by $\vec{E}_0(\vec{r})$]. The filtering is done by convolving the electromagnetic field in time with a bandpass filter centered at the resonant frequency of the fundamental mode and with an appropriate bandwidth [12], [23]. The filtered mode is then normalized in the following way:

$$\iiint_{V_{CD}}\epsilon(\vec{r})|\vec{E}_0(\vec{r})|^2\,d^3\vec{r}=1. \tag{11}$$

Once we have solved for the field pattern of the mode of interest, we then proceed to calculate the electric and magnetic fields of the system excited by oscillating dipoles.

## B. Dipole Sources

Let us assume we have $N$ dipoles, all at the same time in the microcavity, that are randomly positioned and randomly polarized in the active region ($\vec{r}_p^{(i)}$ and $\hat{P}_0^{(i)}$ are the position and the polarization of the $i$th dipole, respectively). We consider dipoles which have a single oscillation frequency $\omega_p$ and lifetime $\tau_d$, but random phases which are uniformly distributed in the range $[0,2\pi)$ ($\phi_i$ is the initial phase of the $i$th dipole).

The Maxwell curl equations now have the following form:

$$\vec{\nabla}\times\vec{H}=\epsilon(\vec{r})\,\frac{\partial\vec{E}}{\partial t}+\frac{\partial\vec{P}}{\partial t} \tag{12}$$

$$\vec{\nabla}\times\vec{E}=-\mu_0\frac{\partial\vec{H}}{\partial t} \tag{13}$$

where $\vec{P}(\vec{r},t)$ is given by the following expression:

$$\vec{P}(\vec{r},t)=\sum_{i=1}^{N}\hat{P}_0^{(i)}e^{j(\omega_p t+\phi_i)}e^{-(t/\tau_d)}\delta(\vec{r}-\vec{r}_p^{(i)}). \tag{14}$$

We discretize (12)–(14) with the initial conditions $\vec{E}(\vec{r},t=0^-)=0$ and $\vec{H}(\vec{r},t=0^-)=0$. Mur's absorbing boundary condition is again applied to the boundaries of the computational domain $V_{CD}$. The electric field in the cavity can be separated into transverse and longitudinal parts [19]

$$\vec{E}(\vec{r},t)=\vec{E}_T(\vec{r},t)+\vec{E}_L(\vec{r},t) \tag{15}$$

where

$$\vec{\nabla}\cdot(\epsilon(\vec{r})\vec{E}_T(\vec{r},t))=0 \tag{16}$$

Using the FDTD method, we evolve real parts of the fields

$$\vec{E}^{\Re}(\vec{r},t)=\Re[\vec{E}(\vec{r},t)] \tag{17}$$

$$\vec{H}^{\Re}(\vec{r},t)=\Re[\vec{H}(\vec{r},t)]. \tag{18}$$

Let us choose a volume $V$ (with outer surface $S$) to be a subset of $V_{CD}$ containing all the dipoles and enclosing the microcavity. At time $t$, we calculate the energy radiated into all modes, $W_\Sigma(t)$, as

$$W_\Sigma(t)=W_{E,V}(t)+W_{H,V}(t)+\int_0^t P_{\mathrm{rad}}(\tau)\,d\tau \tag{19}$$

$$W_{E,V}(t)=\iiint_V\frac{\epsilon(\vec{r})}{2}\,|\vec{E}_T^{\Re}(\vec{r},t)|^2\,d^3\vec{r} \tag{20}$$

$$W_{H,V}(t)=\iiint_V\frac{\mu_0}{2}\,|\vec{H}^{\Re}(\vec{r},t)|^2\,d^3\vec{r} \tag{21}$$

$$P_{\mathrm{rad}}(\tau)=\iint_S(\vec{E}^{\Re}(\vec{r},\tau)\times\vec{H}^{\Re}(\vec{r},\tau))\,d\vec{S} \tag{22}$$

where $P_{\mathrm{rad}}(\tau)$ represents the power radiated out of the cavity and $\vec{E}_T^{\Re}(\vec{r},t)$ is defined as

$$\vec{E}_T^{\Re}(\vec{r},t)=\Re[\vec{E}_T(\vec{r},t)] \tag{23}$$

The total energy radiated into all modes is

$$W_{\Sigma\infty}=\lim_{t\to\infty}W_\Sigma(t). \tag{24}$$

If we evolve the fields for a long enough time $t'$ ($t' \gg \tau_d$) such that the energy of the electromagnetic field which remains within $V$ at $t = t'$ is negligible, we can approximate $W_{\Sigma\infty}$ as

$$W_{\Sigma\infty} = W_\Sigma(t') \approxeq \int_0^{t'} P_{\text{rad}}(\tau)\, d\tau. \tag{25}$$

The transverse electric field (which is the radiation field [18], [19]) can be expressed as the superposition of the complete set of orthonormal modes of the closed cavity $\vec{E}_m(\vec{r})$, introduced previously

$$\vec{E}_T(\vec{r}, t) = \sum_n \vec{E}_n(\vec{r}) g_n(t). \tag{26}$$

$\vec{E}_T(\vec{r}, t)$ satisfies the following wave equation:

$$\begin{aligned}\vec{\nabla} \times [\vec{\nabla} \times \vec{E}_T] = &-2\mu_0 \epsilon(\vec{r}) \sum_m \kappa_m \vec{E}_m(\vec{r}) \dot{g}_m(t) \\ &- \mu_0 \epsilon(\vec{r}) \frac{\partial^2 \vec{E}_T}{\partial t^2} - \mu_0 \frac{\partial^2 \vec{P}_T}{\partial t^2}\end{aligned} \tag{27}$$

where $\vec{P}_T$ denotes the tranverse component of $\vec{P}$. From (3), (5), (26), and (27), we obtain the differential equation for $g_m(t)$, corresponding to a localized mode labeled by index $m$

$$\begin{aligned}\ddot{g}_m(t) &+ \frac{\omega_m}{Q_m} \dot{g}_m(t) + \omega_m^2 g_m(t) \\ &= -\iiint_{V_{CD}} d^3\vec{r} \vec{E}_m^*(\vec{r}) \cdot \frac{\partial^2 \vec{P}_T(\vec{r}, t)}{\partial t^2} \\ &= -\iiint_{V_{CD}} d^3\vec{r} \vec{E}_m^*(\vec{r}) \cdot \frac{\partial^2 \vec{P}(\vec{r}, t)}{\partial t^2}.\end{aligned} \tag{28}$$

The transformation of the integral in the previous equation was proven previously in [19]. The right-hand side in (28) can be written in the following way:

$$\begin{aligned}G_m(t) &= -\iiint_{V_{CD}} d^3\vec{r} \vec{E}_m^*(\vec{r}) \cdot \frac{\partial^2 \vec{P}(\vec{r}, t)}{\partial t^2} \\ &= G^{(m)} e^{j\omega_p t} e^{-(t/\tau_d)}\end{aligned} \tag{29}$$

where

$$G^{(m)} = \left[-\omega_p^2 + \frac{1}{\tau_d^2} - j\frac{2\omega_p}{\tau_d}\right] \sum_{i=1}^{N} \hat{P}_0^{(i)} \vec{E}_m^*(\vec{r}_p^{(i)}) e^{j\phi_i}. \tag{30}$$

Under the condition that the transverse electric field is zero at $t = 0$ ($g_m(0) = 0$ for all $m$), we solve (28) for $g_m(t)$

$$g_m(t) = B_m(e^{j\omega_p t} e^{-(t/\tau_d)} - e^{j\omega_m t} e^{-(\omega_m t/2Q_m)}) \tag{31}$$

$$B_m = \frac{G^{(m)}}{\omega_m^2 - \omega_p^2 + \frac{1}{\tau_d^2} - \frac{\omega_m}{\tau_d Q_m} - j\omega_p\left(\frac{2}{\tau_d} - \frac{\omega_m}{Q_m}\right)}. \tag{32}$$

Let us label the fundamental mode by index 0. Then the energy radiated into the fundamental mode at time $t \to \infty$ can be calculated as [3]

$$W_{0\infty} = \tfrac{1}{2} \int_0^\infty 2\kappa_0\, dt \iiint_{V_{CD}} \epsilon(\vec{r}) \vec{E}_0(\vec{r}, t) \vec{E}_0^*(\vec{r}, t)\, d^3\vec{r} \tag{33}$$

where

$$\vec{E}_0(\vec{r}, t) = \vec{E}_0(\vec{r}) g_0(t). \tag{34}$$

It follows that

$$\begin{aligned}W_{0\infty} = &\kappa_0 |B_0|^2 \\ &\cdot \left[\frac{\tau_d}{2} + \frac{Q_0}{\omega_0} - \frac{2\left(\frac{1}{\tau_d} + \frac{\omega_0}{2Q_0}\right)}{(\omega_p - \omega_0)^2 + \left(\frac{1}{\tau_d} + \frac{\omega_0}{2Q_0}\right)^2}\right]\end{aligned} \tag{35}$$

It should be noted that the choice of $\dot{g}_0(0)$ does not influence the value of $W_{0\infty}$. An alternative approach (which leads to the same result) is to calculate $W_{0\infty}$ in the following way:

$$W_{0\infty} = \int_0^\infty dt \frac{1}{2} \Re\left[\iiint_{V_{CD}} \vec{E}_0^*(\vec{r}, t) \cdot \frac{\partial \vec{P}(\vec{r}, t)}{\partial t} d^3\vec{r}\right]. \tag{36}$$

The $\beta$ factor of the fundamental mode is equal to the ratio of the total energy radiated into that mode and the total energy radiated into all modes [2]–[4].

We include inhomogenous broadening by using an approximate transition spectrum which has a Lorentzian shape, with the central frequency $\omega_s$ and FWHM equal to $\Delta\omega_s$:

$$F(w_p) = \frac{\frac{\Delta\omega_s}{2\pi}}{(\omega_p - \omega_s)^2 + \left(\frac{\Delta\omega_s}{2}\right)^2} \tag{37}$$

$$\int_{-\infty}^{+\infty} F(\omega_p)\, d\omega_p = 1 \tag{38}$$

where $F(w_p)$ represents the density of dipoles (electronic states) at the frequency $w_p$. We average the result over different dipole resonant frequencies

$$\beta = \frac{\sum_{\omega_p} F(\omega_p) W_{0\infty}(\omega_p)}{\sum_{\omega_p} F(\omega_p) W_{\Sigma\infty}(\omega_p)}. \tag{39}$$

The value of the $\beta$ factor when only homogeneous broadening is taken into account and dipoles have the frequency $\omega_p$ is denoted by $\beta_H$ and given by

$$\beta_H = \frac{W_{0\infty}(\omega_p)}{W_{\Sigma\infty}(\omega_p)}. \tag{40}$$

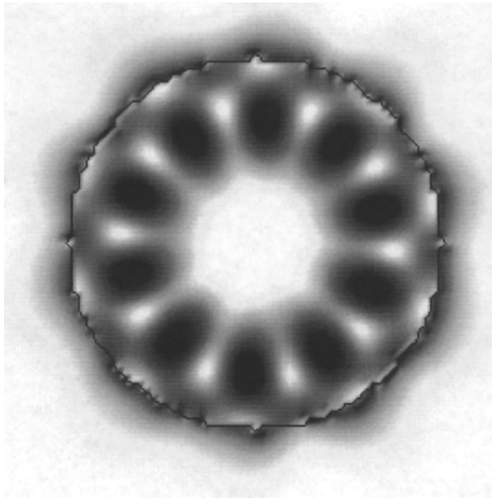

(a)

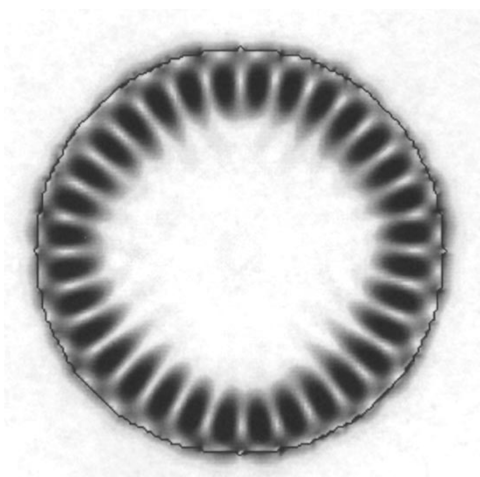

(b)

Fig. 1. (a) Two-dimensional slice through the middle of the microdisk showing (a) the TE(5, 1) mode electric field amplitude and (b) the TE(16, 1) mode electric field amplitude.

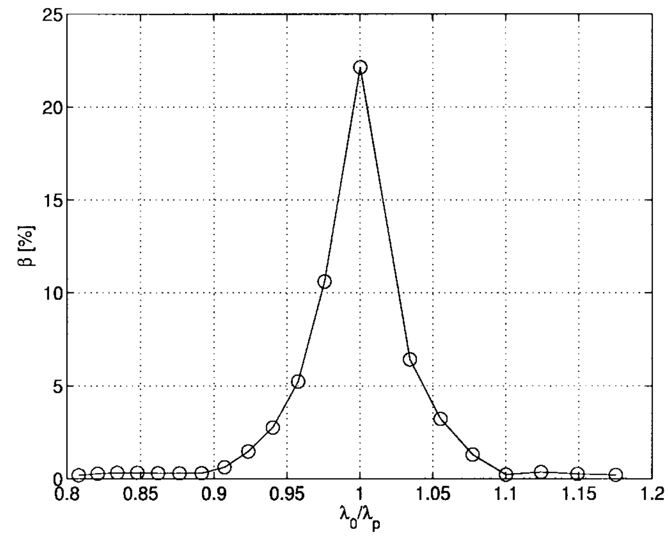


Fig. 2. $\beta_H(\lambda_p)$ for the microdisk laser with $(R/d) = 4.5$ and $(R/\lambda_0) = 0.52$. $\tau_d = 0.1$ ps. On $x$ axis we plot the ratio of the wavelength of the TE(5, 1) mode, $\lambda_0$ and the wavelength of the dipole oscillation $\lambda_p$.

TABLE I
$\beta$ FACTOR CALCULATION FOR THE TE(5, 1) MODE OF THE MICRODISK LASER WITH $(R/d) = 4.5$ AND $(R/\lambda_0) = 0.52$

| $\Delta\lambda_s[nm]$ | $\beta[\%]$ |
|---|---|
| 200 | 11.48 |
| 180 | 12.13 |
| 150 | 13.29 |
| 130 | 14.21 |
| 80 | 17.22 |
| 25 | 22.14 |

## III. $\beta$ FACTOR OF THE MICRODISK LASER

Many analyses, both theoretical and experimental, of the spontaneous emission factor of the microdisk laser can be found in the literature [5], [24]. Using the previously described FDTD method, we calculate the $\beta$ factor of the microdisk and compare our results with the experimental work of Frateschi and Levi [24] and the theoretical work by Chin *et al.* [5].

The parameters used to describe a microdisk are the ratio of its radius and its thickness $R/d$, the ratio of its radius and the wavelength of the fundamental mode $R/\lambda_0$, and the refractive index of the disk $n_{\text{disk}}$. (Note that all wavelengths mentioned throughout this paper are measured in air.)

The first structure that we analyze has the same set of parameters as the structure in [24]: $(R/d) = 4.5$, $(R/\lambda_0) = 0.52$, and $n_{\text{disk}} = 3.4$ (disk is surrounded by air). The fundamental mode (lasing mode) is the TE(5, 1) mode whose electric field pattern, obtained by FDTD, is shown in Fig. 1. In the notation TE$(m, n)$, $m$ denotes the azimuthal number of a mode (there are $2m$ nodes along the $\phi$ direction) and $n$ corresponds to the radial number of a mode ($n-1$ nodes along the radial direction). For a lasing wavelength of the TE(5, 1) mode equal to $\lambda_0 = 1.55$ $\mu$m, parameters of the disk are $R = 0.8$ $\mu$m and $d = 0.18$ $\mu$m. We calculate the quality factor of the TE(5, 1) mode to be $Q_0 = 740$. This is much larger than the calculated value of [24] due to the fact that we neglect absorption losses and the presence of the post. For the purpose of calculating the $\beta$ factor, we consider the active layer (quantum well) to be centered in the middle of the disk. We assume that the quantum well (QW) couples most strongly to TE modes, so we only consider oscillating dipoles with polarization in the plane of the QW. Dipoles appear uniformly throughout the area of the disk. The calculated values of $\beta_H$ ($\tau_d = 0.1$ ps, which corresponds to a FWHM of the emission spectrum equal to 25 nm at $\lambda_0 = 1.55$ $\mu$m) for different wavelengths of the dipole excitation $\lambda_p$ are shown in Fig. 2.

In order to account for the inhomogeneous broadening, the emission spectrum from the QW is approximated by a Lorentzian, centered at the wavelength equal to $\lambda_s$ and with FWHM denoted by $\Delta\lambda_s$. We analyze several possibilities for $\Delta\lambda_s$ and assume that $\lambda_s = \lambda_0 = 1.55$ $\mu$m. The results are shown in Table I. The first row corresponds to the condition in [24] where the experimentally observed value of $\beta$ was 4.5%. It should be noted that in our calculation $\beta$ is averaged over a finite frequency range which neglects the long tails of

TABLE II
$\beta_H$ FACTOR CALCULATION FOR THE MICRODISK LASERS WHEN $\lambda_0 = \lambda_s = 1.55\ \mu$m AND $\Delta\lambda_s = 0.016\lambda_s = 25$ nm

| $\frac{R}{d}$ | $\frac{R}{\lambda_0}$ | mode | $Q$ | $\beta_H[\%]$ | $N_g$ | $\rho[nm^{-1}]$ |
|---|---|---|---|---|---|---|
| 8.3 | 1.2 | TE(16,1) | 2879 | 2.88 | 2 | 1.3 |
| 4.5 | 0.52 | TE(5,1) | 740 | 22.14 | 2 | 0.1 |
| 1.5 | 0.44 | TE(5,1) | 1293 | 30.56 | 2 | 0.05 |

the Lorentzian. This leads to a small overestimation of $\beta$. We also neglect the presence of the post as well as absorption losses, which causes the additional discrepancy.

We analyze two more microdisk structures, whose parameters and calculated $\beta$ values are shown in Table II. The pattern of the TE(16, 1) mode, which was analyzed in one of the microdisks, is given in Fig. 1. In [5], the simplified model of modes of the microdisk and the mode density leads to overestimated $\beta$ values, as noted previously [25].

In order to separate the contribution of guided modes and radiation modes to the $\beta$ factor, one can use the following approximate expression:

$$\beta = \frac{1}{N_g + \rho\Delta\lambda_s} \tag{41}$$

where $\Delta\lambda_s$ is the width of the spontaneous emission spectrum, $N_g$ is the number of guided modes within the spontaneous emission spectrum, and $\rho$ is an effective density of radiation modes at $\lambda_s$. In (41), it is assumed that the same amount of spontaneous emission goes into all guided modes within the emission spectrum and that the density of radiation modes is constant within $\Delta\lambda_s$. $N_g$ can be counted from the spectrum determined using the FDTD (as described in Section II). The values of $N_g$ and $\rho$ for the analyzed microdisk structures are given in Table II.

## IV. $\beta$ FACTOR OF THE MICROCAVITY BASED ON 2-D PBG IN AN OPTICALLY THIN DIELECTRIC SLAB

Optical microcavities can be constructed by introducing defects into photonic crystals [8], [26]. These microcavities support high-$Q$, localized modes (defect modes), which have their resonant frequencies within the bandgap of the photonic crystal.

The microcavity that we analyze is an optically thin dielectric slab patterned with a 2-D array of holes, as shown in Fig. 3. A defect is made by omitting a central hole in the 2-D array of air holes. A 2-D PBG is used to laterally confine the defect mode and to suppress the lateral radiation. Total internal reflection at the air–membrane boundary is used for vertical confinement of the mode. The important parameters of the structure are the distance between the centers of adjacent air holes $a$, the radius of an air hole $r$, the number of periods of holes around the defect $n_{\mathrm{per}}$, the thickness of the membrane $d$, and the refractive index of the membrane $n_{\mathrm{slab}}$. The parameters of the analyzed structure are $(r/a) = 0.3$, $(d/a) = 0.4$, $n_{\mathrm{slab}} = 3.4$, and $n_{\mathrm{per}} = 3$. The detailed analysis of localized defect modes in this structure was presented in [12]. In Fig. 4, we show the top view of a microfabricated defect cavity in InGaAsP, designed for 1.55-$\mu$m emission [27].

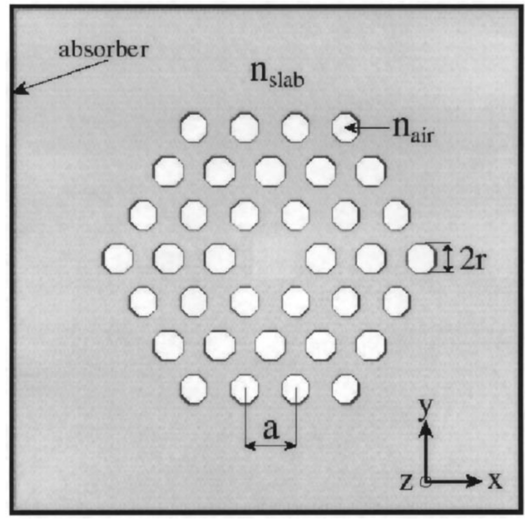


Fig. 3. Schematic of a 2-D slice through the middle of the patterned high-index slab. A defect in the hexagonal lattice of the air holes is formed by omitting the central hole of the array.

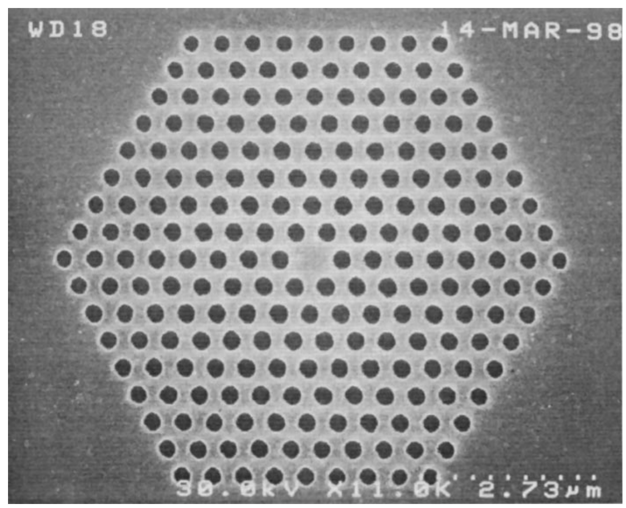


Fig. 4. Top view of a microfabricated 2-D hexagonal array of holes with a single central hole missing. The interhole spacing is $a = 500$ nm and the radius of the holes is approximately 150 nm.

The defect modes are a set of doubly degenerate dipole modes shown in Fig. 5, which we term the $x$-dipole and $y$-dipole modes in reference to the fact that they transform like the $x$ and $y$ components of a vector under the point group operations of $C_{6v}$ [12]. We consider the $y$-dipole mode to be the fundamental mode. The normalized frequency of the fundamental mode is $(a/\lambda_0) = 0.32$ and its quality factor is $Q_0 = 129$. If we assume that in reality $\lambda_0 = 1.55\ \mu$m, this corresponds to $d = 198$ nm, $a = 495$ nm, and $r = 165$ nm. The bandgap of the infinite 2-D photonic crystal of this thickness extends from $(a/\lambda) = 0.2983$ to $(a/\lambda) = 0.3884$ [12].

The active layer (QW) is again centered in the middle of the dielectric membrane. We assume that the QW couples most strongly to TE modes, so we only analyze dipoles with the

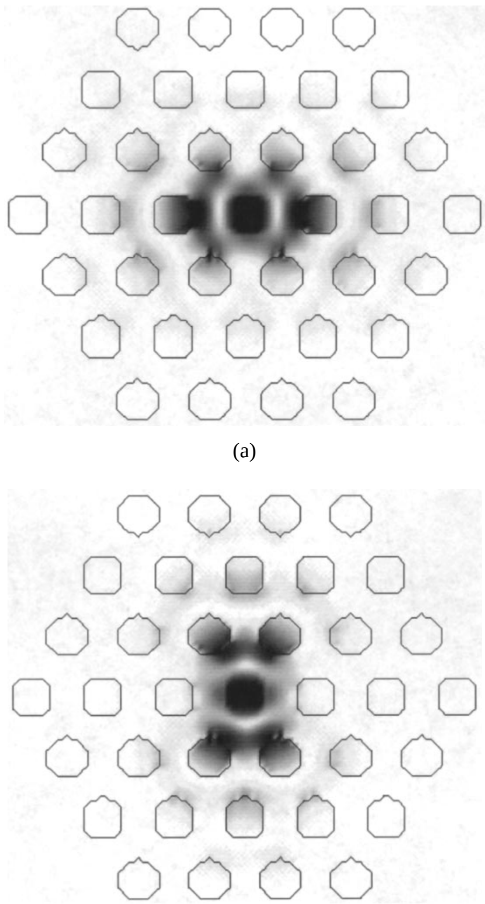

(a)

(b)

Fig. 5. (a) Two-dimensional slice through the middle of the slab showing the $x$ dipole mode electric field amplitude. (b) $y$ dipole mode electric field amplitude.

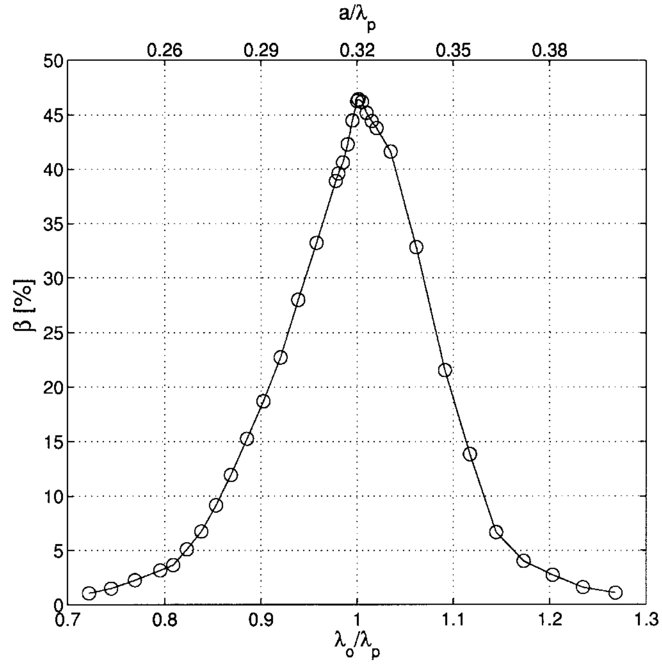


Fig. 6. $\beta_H$ dependence on the wavelength of the dipole excitation $\lambda_p$ for the microcavity based on 2-D PBG. $\lambda_0$ is the wavelength of the $y$-dipole mode. $\tau_d = 0.1$ ps.

TABLE III
$\beta$ FACTOR CALCULATION FOR THE $y$-DIPOLE MODE OF THE MICROCAVITY BASED ON 2-D PBG IN AN OPTICALLY THIN DIELECTRIC SLAB; PARAMETERS OF THE CAVITY ARE DESCRIBED IN THE TEXT

| $\lambda_0[nm]$ | $\lambda_s[nm]$ | $\Delta\lambda_s[nm]$ | $\beta[\%]$ |
|---|---|---|---|
| 1550 | 1550 | 200 | 40 |
| 1550 | 1550 | 150 | 41.26 |
| 1550 | 1550 | 130 | 41.7 |
| 1550 | 1550 | 80 | 43 |
| 1550 | 1550 | 25 | 46.42 |

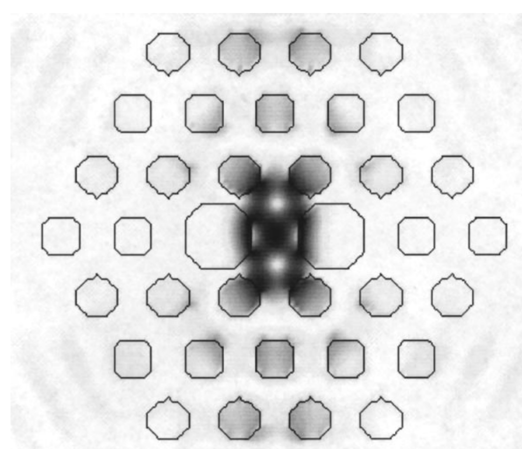

Fig. 7. Cavity geometry for splitting of the dipole mode degeneracy and 2-D slice through the middle of the slab showing the $y$-dipole mode electric field amplitude.

polarization in the plane of the QW. Dipoles appear uniformly throughout the the area of the defect. The lifetime of dipoles is assumed to be $\tau_d = 0.1$ ps.

The results of $\beta_H$ for different dipole wavelengths $\lambda_p$ are shown in Fig. 6. In order to account for the inhomogeneous broadening, we approximate the emission spectrum from the QW by a Lorentzian, centered at $\lambda_s$ and with FWHM denoted by $\Delta\lambda_s$. Using the averaging technique described in Section II, we calculate the value of the $\beta$ factor for different values of the inhomogeneous broadening and the central frequency of the spectrum matched to the frequency of the fundamental mode. The results are given in Table III.

For $\Delta\lambda_s = 25$ nm, $N_g = 2$ (doubly degenerate fundamental mode), and $\beta_H = 46.42\%$, we calculate the effective density of radiation modes to be $\rho = 0.006\,17$ nm$^{-1}$ which is around ten times smaller than in the microdisk which has a peak value of $\beta = 30.56\%$. We attribute such a small $\rho$ to the suppression of radiation modes by the 2-D photonic crystal over a finite in-plane angular range.

The $\beta$ factor can be almost doubled using the degeneracy splitting of the dipole modes. Degeneracy splitting can be accomplished by lowering the defect symmetry relative to that of the hexagonal lattice (as an example, by increasing the radius of the two nearest neighbor holes along the $x$ axis) [12]. In the previously analyzed PBG membrane, we increase the radii of the two nearest neighbor holes to $0.5a$ and move them $0.2a$ simultaneously toward the center defect in order to maintain the rib size in the $x$ direction. We analyze the $\beta$ factor of the $y$-dipole mode (shown in Fig. 7), whose parameters are $Q = 224$ and $(a/\lambda_0) = 0.34$. For $\lambda_s = \lambda_0 = 1.55\ \mu$m and $\Delta\lambda_s = 25$ nm, we obtain $\beta = 86.82\%$.

## V. Conclusions

We proposed a new method for the calculation of the spontaneous emission coupling factor using the finite-difference time-domain method. We calculated the $\beta$ factor of the microdisk laser and compared it with existing theoretical and experimental data. We also calculated $\beta$ of the microcavity based on the 2-D PBG structure. We conclude that the latter structure is a promising design for a very low threshold laser, since the 2-D PBG suppresses the in-plane radiation modes. We estimate that the $\beta$ factor can be as large as 87% (when degeneracy is broken) for a 2-D PBG defect.

## Acknowledgment

The authors would like to thank M. Lončar for many helpful suggestions.

## References

[1] G. Björk and Y. Yamamoto, "Analysis of semiconductor microcavity lasers using rate equations," *IEEE J. Quantum Electronics*, vol. 27, pp. 2386–2396, Nov. 1991.

[2] Y. Suematsu and K. Furuya, "Theoretical spontaneous emission factor of injection lasers," *Trans. IECE Japan*, vol. E60, no. 9, pp. 467–472, Sept. 1977.

[3] T. Baba, T. Hamano, F. Koyama, and K. Iga, "Spontaneous emission factor of a microcavity DBR surface-emitting laser," *IEEE J. Quantum Electron.*, vol. 27, pp. 1347–1358, June 1991.

[4] ——, "Spontaneous emission factor of a microcavity DBR surface-emitting laser (II)—Effects of electron quantum confinements," *IEEE J. Quantum Electron.*, vol. 28, pp. 1310–1319, May 1992.

[5] M. K. Chin, D. Y. Chu, and S. T. Ho, "Estimation of the spontaneous emission factor for microdisk lasers via the approximation of whispering gallery modes," *J. Appl. Phys.*, vol. 75, no. 7, pp. 3302–3307, Apr. 1994.

[6] D. Y. Chu and S. T. Ho, "Spontaneous emission from excitons in cylindrical dielectric waveguides and the spontaneous-emission factor of microcavity ring lasers," *J. Opt. Soc. Amer. B*, vol. 10, no. 2, pp. 381–390, Feb. 1993.

[7] E. Yablonovitch, "Phontonic band gap structures," *J. Opt. Soc. Amer. B*, vol. 10, no. 2, pp. 283–295, Feb. 1993.

[8] J. D. Joannopoulos, R. D. Meade, and J. N. Winn, *Photonic Crystals*. Princeton, NJ: Princeton Univ., 1995.

[9] P. Villeneuve and M. Piché, "Photonic bandgaps in periodic dielectric structures," *Prog. Quantum Electron.*, vol. 18, pp. 153–200, 1994.

[10] P. Villeneuve, S. Fan, and J. D. Joannopoulos, "Microcavities in phontonic crystals: Mode symmetry, tunability and coupling efficiency," *Phys. Rev. B*, vol. 54, no. 11, pp. 7837–7842, Sept. 1996.

[11] ——, "Air-bridge microcavities," *Appl. Phys. Lett.*, vol. 67, no. 2, pp. 167–169, July 1995.

[12] O. Painter, J. Vuč, and A. Scherer, "Defect modes of a two-dimensional phontonic crystal in an optically thin dielectric slab," *J. Opt. Soc. Amer. B*, vol. 16, no. 2, pp. 275–285, Feb. 1999.

[13] E. Yablonovitch, "Inhibited spontaneous emission in solid-state physics and electronics," *Phys. Rev. Lett.*, vol. 58, no. 20, pp. 2059–2062, May 1987.

[14] H. Yokoyama, "Physical and device applications of optical microcavities," *Science*, vol. 256, pp. 66–70, Apr. 1992.

[15] K. S. Lee, "Numerical solution to initial boundary value problems involving Maxwell's equations in isotropic media," *IEEE Trans. Antennas Propagat.*, vol. AP-14, pp. 302–307, May 1966.

[16] A. Taflove, *Computational Electrodynamics—The Finite-Difference Time-Domain Method*. Boston, MA: Artech House, 1995.

[17] A. E. Siegman, *Lasers*. Mill Valley, CA: University Science, 1986.

[18] E. A. Hinds, "Perturbatice cavity quantum electrodynamics," *Cavity QED*, P. R. Berman, Ed.. New York: Academic, 1994, pp. 1–55.

[19] R. J. Glauber and M. Lewenstein, "Quantum optics of dielectric media," *Phys. Rev. A*, vol. 43, no. 1, pp. 467–491, 1991.

[20] Y. Xu, J. Vuč, R. K. Lee, O. J. Painter, A. Scherer, and A. Yariv, "Finite-difference time-domain calculation of spontaneous emission lifetime in a microcavity," *J. Opt. Soc. Amer. B*, vol. 16, no. 3, pp. 465–474, 1999.

[21] A. Yariv, *Optical Electronics in Modern Communications*. New York: Oxford Univ., 1997.

[22] G. Mur, "Absorbing boundary conditions for the finite-difference approximation of the time-domain electromagnetic-field equations," *IEEE Trans. Electromag. Compat.*, vol. EMC-23, pp. 377–382, Nov. 1981.

[23] D. H. Choi and W. J. R. Hoefer, "The finite-difference-time-domain method and its application to eigenvalue problems," *IEEE Trans. Microwave Theory Tech.*, vol. 34, pp. 1464–1469, Dec. 1986.

[24] N. C. Frateschi and A. F. J. Levi, "The spectrum of microdisk lasers," *J. Appl. Phys.*, vol. 80, no. 2, pp. 644–653, July 1996.

[25] G. Chang-Zhi and C. Shui-Lian, "Whispering-gallery mode structure in semiconductor microdisk lasers and control of the spontaneous emission factor," *Acta Physica Sinica (Overseas Edition)*, vol. no. 3, pp. 185–194, 1996.

[26] H. A. Haus and C. V. Shank, "Antisymmetric taper of distributed feedback lasers," *IEEE J. Quantum Electron.*, vol. QE-12, p. 532, 1976.

[27] O. Painter, R. Lee, A. Yariv, A. Scherer, and J. O'Brien, "Photonic bandgap membrane microresonator," *Integr. Photon. Res.*, vol. 4, pp. 221–223, 1998.

**Jelena Vučković** (S'99) was born in Niš, Yugoslavia, in 1971. She received the B.S.E.E. degree from the University of Niš, Yugoslavia, in 1993 and the M.S. degree in electrical engineering from California Institute of Technology, Pasadena, in 1997, where she is currently working toward the Ph.D. degree.

During 1994 and 1995, she worked as a Research and Teaching Assistant at the University of Niš and, during 1996, as a Researcher at the School of Electrical Engineering, University of Sydney, Australia. Her research interests include optical microcavities, spontaneous emission control, and photonic crystals.

**Oskar Painter** (S'99) was born in Toronto, Canada, in 1972. He received the B.S.E.E. degree from the University of British Columbia in 1994 and the M.S. degree in electrical engineering from the California Institute of Technology, Pasadena, in 1995, where he is currently working toward the Ph.D. degree.

His research interests include design and fabrication of novel optical microcavities, photonic crystals, and ultrasmall device processing techniques.

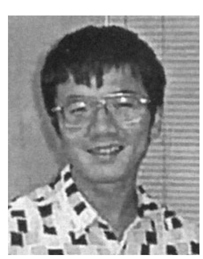

**Yong Xu** was born in Beijing, China on November 25, 1974. He received the B.S. degree in applied physics from Tsinghua University, China, in 1995. He is currently completing the Ph.D. degree in physics at the California Institute of Technology, Pasadena.

His research interests include computational electromagnetics and integrated photonic devices.

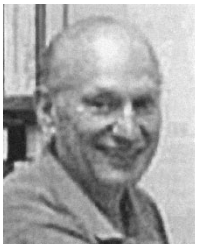

**Amnon Yariv** (S'56–M'59–F'70–LF'95) received the B.S., M.S., and Ph.D. degrees from the University of California, Berkeley, in 1954, 1956, and 1958, respectively.

He is a Martin and Eileen Summerfield Professor of Electrical Engineering and Professor of Applied Physics at California Institute of Technology. His research interests include semiconductor lasers physics, dynamics of semiconductor lasers, effect of dispersive propagation in fibers on intensity noise and modulation response of semiconductor lasers, photonic bandgap phenomena and devices and WDM filters.

Dr. Yariv is one of the founders of the field of optoelectronics and a member of the National Academy of Engineering and the National Academy of Sciences.

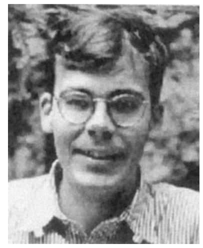

**Axel Scherer** received the B.S., M.S., and Ph.D. degrees from the New Mexico Institute of Mining and Technology in 1981, 1982, and 1985, respectively.

From 1985 until 1993, he worked in the Quantum Device Fabrication group at Bellcore. Currently, he is Professor of Electrical Engineering, Applied Physics, and Physics at the California Institute of Technology, Pasadena, specializing in device microfabrication. His research interests include design and fabrication of functional photonic, nanomagnetic, and microfluidic devices.